

*Engineering*

*Industrial & Management Engineering fields*

---

Okayama University

Year 1995

---

Visual servoing with nonlinear observer

Koichi Hashimoto  
Okayama University

Hidenori Kimura  
Osaka University

This paper is posted at eScholarship@OUDIR : Okayama University Digital Information Repository.

<http://escholarship.lib.okayama-u.ac.jp/industrial-engineering/100>

# Visual Servoing with Nonlinear Observer

Koichi Hashimoto

Department of Mechanical Engineering  
Okayama University  
3-1-1 Tsushima-naka, Okayama 700 JAPAN  
koichi@mcrlab.mech.okayama-u.ac.jp

Hidenori Kimura

Department of Systems Engineering  
Osaka University  
1-1 Machikaneyama, Toyonaka 560 JAPAN  
kimura@sys.es.osaka-u.ac.jp

## Abstract

Visual servo system is a robot control system which incorporates the vision sensor in the feedback loop. Since the robot controller is also in the visual servo loop, compensation of the robot dynamics is important for high speed tasks. Moreover estimation of the object motion is necessary for real time tracking because the visual information includes considerable delay. This paper proposes a nonlinear model-based controller and a nonlinear observer for visual servoing. The observer estimates the object motion and the nonlinear controller makes the closed loop system asymptotically stable based on the estimated object motion. The effectiveness of the observer-based controller is verified by simulations and experiments on a two link planar direct drive robot.

## 1 Introduction

Visual information on tasks and environments is essential to execute flexible and autonomous tasks. Tracking the object with the robot hand based on the visual information is called visual tracking. Visual tracking has some technical problems such as delay, low sampling frequency, nonlinear perspective transformation and nonlinear robot dynamics.

Visual servo systems incorporate the visual sensors in the feedback loop. As shown in Figure 1, the joint servo loop of the robot is also incorporated in the visual feedback loop. Thus the performance of the outer visual loop may be deteriorated by the poor performance of the inner joint servo loop. However previous studies [12, 5, 7, 4, 11] assumed the ideal performance of the joint servo mechanism and ignored the robot dynamics.

Due to the low frequency of the visual sampling, estimation of the object motion is also essential for visual tracking. Since the visual sampling period is larger than 33 ms, significant delay is inevitable without predictive control. Studies on object motion estimation based on Kalman filter and AR model were carried out by Koivo

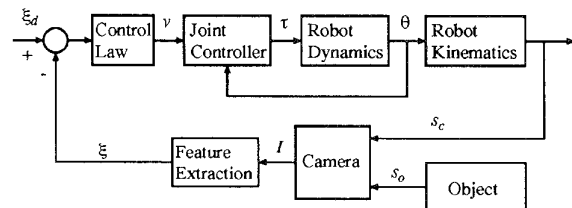


Figure 1: Feature-based Visual Tracking

and Houshangi [10], Corke and Good [3], Wilson [13], Chaumette and Santos [2] and Allen *et al.*[1]. However, they did not model the object motion and did not consider the robot dynamics. Though Ghosh *et al.*[6] proposed a model-based nonlinear estimator, the control problem was not considered.

This paper proposes a nonlinear controller and a nonlinear observer for visual tracking. A model describing the object motion is proposed and the nonlinear observer estimates the velocity parameters of the object motion model. The nonlinear controller compensates the robot dynamics based on the object velocity estimation. The proposed controller is proved to be asymptotically stable. Thus the tracking error converges to zero. The effectiveness of the proposed method is evaluated by simulations and experiments on a two link planar direct drive robot. The results exhibit the fast convergence of the estimator and the accurate tracking performance of the controller.

## 2 Models

The objective of this paper is to track a moving object by a hand-mounted camera based on the visual information. As depicted in Figure 2, let the camera and the object position and orientation be  $s_c \in \mathbf{R}^6$  and  $s_o \in \mathbf{R}^6$ , respectively. Then, for the given desired relative position and orientation  $\sigma_d \in \mathbf{R}^6$ , **tracking** is defined by

$$\sigma \equiv \sigma_d, \quad \sigma \stackrel{\text{def}}{=} s_c - s_o. \quad (1)$$

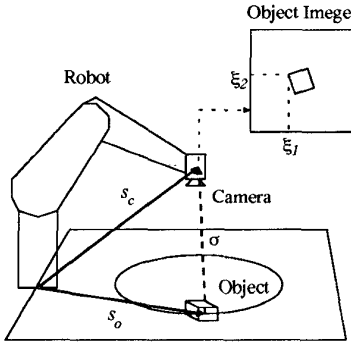


Figure 2: Visual Tracking

## 2.1 Robot Model

Assume that the robot has  $m$  ( $\leq 6$ ) joints. The **dynamic model of robot** is given by

$$\frac{d}{dt} \begin{bmatrix} q \\ \dot{q} \end{bmatrix} = \begin{bmatrix} \dot{q} \\ -M^{-1}h \end{bmatrix} + \begin{bmatrix} 0 \\ M^{-1} \end{bmatrix} \tau, \quad (2)$$

where  $q$  is the joint angle vector,  $\tau$  is the actuator torque vector,  $M$  is the inertia matrix, and  $h$  is the vector representing the Coriolis, centrifugal and gravity forces.

## 2.2 Camera Model

Assume that the object image is represented by an  $n$  dimensional feature vector  $\xi$ , which is a function of the relative position and orientation between object and camera  $\sigma = s_c - s_o$ . Let the feature vector satisfying  $\sigma = \sigma_d$  be the desired feature vector  $\xi_d$ . Then the **camera model** is expressed by the mapping  $\iota: \mathbf{R}^6 \rightarrow \mathbf{R}^n$  defined by

$$\xi \stackrel{\text{def}}{=} \iota(\sigma), \quad \iota(\sigma_d) = \xi_d. \quad (3)$$

**Example** A planar two link robot example is shown in Figure 3. The camera is mounted on the second link looking upward. Let  $\ell_1$  be the link 1 length and  $[\ell_{cx} \ \ell_{cy}]^T$  be the camera position with respect to the link 2. Then we have the camera position and orientation

$$s_c = \left. \begin{array}{l} \left. \begin{array}{l} \ell_1 c_1 + \ell_{cx} c_{12} - \ell_{cy} s_{12} \\ \ell_1 s_1 + \ell_{cx} s_{12} + \ell_{cy} c_{12} \\ Z_c \\ 0 \\ 0 \\ \theta_1 + \theta_2 \end{array} \right\} \text{position} \\ \left. \begin{array}{l} \\ \\ \\ \\ \end{array} \right\} \text{orientation} \end{array} \right\} \quad (4)$$

where  $s_1 = \sin q_1$ ,  $c_1 = \cos q_1$ ,  $s_{12} = \sin(q_1 + q_2)$ ,  $c_{12} = \cos(q_1 + q_2)$ . Assume that an object is above the camera and its position is  $s_o = [X_{obj} \ Y_{obj} \ Z_{obj} \ 0 \ 0 \ 0]^T$ , where the depth  $Z = Z_{obj} - Z_c$  is known. Let the feature

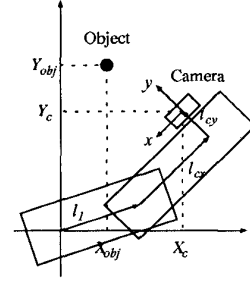


Figure 3: Two Link Direct Drive Robot (overview)

vector  $\xi = [x \ y]^T$  be the position of the object in the image plane,  $f$  be the focal length of the lens,  $\sigma_i$  be the  $i$ th element of  $\sigma$ . Then the object position with respect to the camera coordinate system is given by

$$\begin{bmatrix} {}^c X_{rel} \\ {}^c Y_{rel} \\ {}^c Z_{rel} \end{bmatrix} = \begin{bmatrix} -\cos \sigma_6 & -\sin \sigma_6 & 0 \\ -\sin \sigma_6 & -\cos \sigma_6 & 0 \\ 0 & 0 & -1 \end{bmatrix} \begin{bmatrix} \sigma_1 \\ \sigma_2 \\ \sigma_3 \end{bmatrix}. \quad (5)$$

Therefore we have the camera model

$$\xi = \frac{f}{{}^c Z_{rel}} \begin{bmatrix} {}^c X_{rel} \\ {}^c Y_{rel} \end{bmatrix} = \iota(\sigma). \quad (6)$$

Another representation is obtained by substituting  $\sigma_i$  into (6) as follows

$$\xi = F \begin{bmatrix} \ell_{cx} + \ell_1 c_2 + \alpha \\ -\ell_{cy} + \ell_1 s_2 + \beta \end{bmatrix}, \quad (7)$$

where  $F = \frac{f}{Z}$ ,  $s_2 = \sin q_2$ ,  $c_2 = \cos q_2$  and

$$\alpha = -X_{obj} c_{12} - Y_{obj} s_{12}, \quad \beta = -X_{obj} s_{12} + Y_{obj} c_{12}. \quad (8)$$

## 2.3 Object Motion Model

Assume that the object has  $m_o$  ( $\leq 6$ ) degrees of freedom and let  $p \in \mathbf{R}^{m_o}$  be the generalized coordinates of the object position and orientation. Also assume that the object speed is generated by  $\ell$  ( $\leq m_o$ ) dimensional parameter vector  $\theta^*$  such that

$$\dot{p} = W(p)\theta^* \quad (9)$$

is satisfied, where  $W(p)$  is an  $m_o \times \ell$  matrix function of  $p$ . The vector  $\theta^*$  and the equation (9) are called the **velocity parameter** and the **object motion model**. This motion model is simple but it can model fairly large range of autonomous motions including straight, circular, oval and "figure 8" motions.

The robot configuration should avoid singular points while tracking. Thus we restrict the robot configuration

in a region  $\mathcal{V} \subset \mathbf{R}^6$  which does not contain a singular point. Also we assume that for all  $p \in \mathcal{U}$ , where  $\mathcal{U}$  is a subset of  $\mathbf{R}^{m_o}$  which contains all solutions of (9), the solution  $q^*$  of  $s_c(q^*) = s_o(p) + \sigma_d$  is in  $\mathcal{V}$ . This is a necessary condition for object tracking. To satisfy this condition  $m \geq m_o$  is necessary.

**Example** In the previous example the object height is constant. Thus the object degree of freedom is 2 and the object position is uniquely defined by  $p = [X_{obj} \ Y_{obj}]^T$ .

If the object motion is straight and the object speed in  $X$  and  $Y$  directions are  $v_X$  and  $v_Y$ , respectively, we have (9) with

$$W(p) = I, \quad \theta^* = [v_X \ v_Y]^T. \quad (10)$$

If the object motion is circular with constant velocity  $\omega$ , the object position is described by

$$\begin{bmatrix} X_{obj} \\ Y_{obj} \end{bmatrix} = \begin{bmatrix} r \cos \omega t \\ r \sin \omega t \end{bmatrix}. \quad (11)$$

Thus the object speed is given by (9) with

$$W(p) = \begin{bmatrix} -Y_{obj} \\ X_{obj} \end{bmatrix}, \quad \theta^* = \omega. \quad (12)$$

For “figure 8” motion, the object position becomes

$$\begin{bmatrix} X_{obj} \\ Y_{obj} \end{bmatrix} = \begin{bmatrix} r_1 \cos \omega t \\ r_2 \sin 2\omega t \end{bmatrix}. \quad (13)$$

Then the motion is modeled by (9) with

$$W(p) = \begin{bmatrix} 0 & -\frac{Y_{obj}}{X_{obj}^2} \\ X_{obj}^2 & -\frac{Y_{obj}}{X_{obj}^2} \end{bmatrix}, \quad \theta^* = \begin{bmatrix} \frac{1}{r} \omega \\ r \omega \end{bmatrix}, \quad (14)$$

where  $r = \frac{r_1^2}{2r_2}$ .

### 3 Conditions for Good Features

Features must give enough information to track the object. The derivative of (3) gives

$$\dot{\xi} = J\dot{q} + L\dot{p}, \quad (15)$$

where

$$J \stackrel{\text{def}}{=} \frac{\partial l}{\partial \sigma} \frac{\partial \sigma}{\partial q}, \quad L \stackrel{\text{def}}{=} \frac{\partial l}{\partial \sigma} \frac{\partial \sigma}{\partial p}. \quad (16)$$

The matrices  $J$  and  $L$  are called **image Jacobian** and **motion Jacobian**, respectively. The features must satisfy the following conditions for all  $q \in \mathcal{V}$  and  $p \in \mathcal{U}$

$$\text{rank } J = m, \quad \text{rank } L = m_o. \quad (17)$$

In other words, features must change when either of the robot or the object moves. To satisfy this condition  $n \geq m$  is necessary,<sup>1</sup> and the maximum number of the features is not limited. The maximum should be decided depending on the speed of the image processing.

**Example** For the two link robot example, derivative of (6) is given by (15) with

$$J = F \begin{bmatrix} -\beta & -\ell_1 s_2 - \beta \\ \alpha & \ell_1 c_2 + \alpha \end{bmatrix}, \quad L = F \begin{bmatrix} -c_{12} & -s_{12} \\ -s_{12} & c_{12} \end{bmatrix}. \quad (18)$$

It is easy to see

$$\det J = F^2 \ell_1 (X_{obj} s_1 - Y_{obj} c_1), \quad \det L = -F^2. \quad (19)$$

Thus,  $J$  becomes singular only if the object is on the line connecting the first and second joints, and  $L$  is always nonsingular. To avoid the singular configuration one may select more features than necessary. An example with the redundant features is found in [9].

### 4 Control Law

The models of robot, camera and object motion are given by (2), (3) and (9), respectively. To derive the control law define the controlled variable

$$z \stackrel{\text{def}}{=} B^T (\xi - \xi_d), \quad \xi_d = u(s_c(q^*) - s_o(p^*)), \quad (20)$$

where

$$B \stackrel{\text{def}}{=} \begin{cases} J(q^*, p^*) & \text{if } n > m, \\ I & \text{if } n = m \end{cases}, \quad (21)$$

$p^*$  is a typical object pose and  $q^*$  is the corresponding joint angle which is the solution of  $s_c(q^*) = s_o(p^*) + \sigma_d$ . Taking the second derivative of  $z$  gives

$$\ddot{z} = B^T J M^{-1} (\tau - h) + \lambda + N \theta^* + \Phi \kappa(\theta^*), \quad (22)$$

where

$$\lambda = \begin{bmatrix} \lambda_1 \\ \vdots \\ \lambda_m \end{bmatrix}, \quad N = \begin{bmatrix} N_1 \\ \vdots \\ N_m \end{bmatrix}, \quad \Phi = \begin{bmatrix} \Phi_1 \\ \vdots \\ \Phi_m \end{bmatrix}, \quad (23)$$

and

$$\begin{aligned} \lambda_i &\stackrel{\text{def}}{=} \dot{q}^T \frac{\partial^2 z_i}{\partial q^2} \dot{q}, \quad N_i \stackrel{\text{def}}{=} 2 \dot{q}^T \frac{\partial^2 z_i}{\partial p \partial q} W, \\ \Phi_{ijk} &\stackrel{\text{def}}{=} \left[ \frac{\partial}{\partial p} \left\{ W^T \left( \frac{\partial z_i}{\partial p} \right)^T \right\} W \right]_{jk}, \\ \Phi_i &\stackrel{\text{def}}{=} [ \Phi_{i11} \ \cdots \ \Phi_{i1\ell} \ \Phi_{i21} \ \cdots \ \Phi_{i\ell\ell} ], \\ \kappa(\theta^*) &\stackrel{\text{def}}{=} [ \theta_1^{*2} \ \cdots \ \theta_1^* \theta_\ell^* \ \theta_2^* \theta_1^* \ \cdots \ \theta_\ell^{*2} ]^T. \end{aligned} \quad (24)$$

<sup>1</sup>  $m \geq m_o$  is necessary to track all object pose.

Since  $B$  is full rank and  $J$  is a continuous function of  $p$  and  $q$ ,  $B^T J$  is invertible if  $p$  and  $q$  are close to  $p^*$  and  $q^*$ . Therefore, the actuator torque with new input  $v$

$$\tau = M(B^T J)^{-1}(v - \lambda - N\theta^* - \Phi\kappa(\theta^*)) + h \quad (25)$$

yields a linear dynamics  $\ddot{z} = v$ . Thus we obtain the following theorem.

**Theorem 1** Define the new input  $v$  by

$$v = -K_1 z - K_2 \dot{z}, \quad (26)$$

where  $K_1, K_2$  are positive definite gain matrices. Then the equilibrium point  $(z, \dot{z}) = 0$  becomes exponentially stable by using the nonlinear input transformation (25).

**Example** For the two link robot example, suppose that  $\xi_d = [0 \ 0]^T$ . If the distance from the object to the origin of the work space is close to  $\ell_1$ , the second joint angle is close to  $\pi/2$  and the configuration is far from singular. For simplicity we consider such task and assume that  $J$  is invertible. Since  $n = m = 2$ ,  $B = I$  and  $z = \xi$ .

If the object motion is straight, the object motion model is (10) and we have

$$\begin{aligned} \ddot{z} &= J\ddot{q} + \lambda + N \begin{bmatrix} v_X \\ v_Y \end{bmatrix}, \\ \lambda &= \left[ (\dot{q}_1 + \dot{q}_2) \begin{bmatrix} 0 & -1 \\ 1 & 0 \end{bmatrix} J + F\ell_1 \dot{q}_1 \begin{bmatrix} 0 & c_2 \\ 0 & s_2 \end{bmatrix} \right] \dot{q}, \\ N &= 2F(\dot{q}_1 + \dot{q}_2) \begin{bmatrix} s_{12} & -c_{12} \\ -c_{12} & -s_{12} \end{bmatrix}. \end{aligned} \quad (27)$$

Thus we obtain the controller

$$\tau = MJ^{-1}(-K_1 z - K_2 \dot{z} - \lambda - N \begin{bmatrix} v_X \\ v_Y \end{bmatrix}) + h. \quad (28)$$

If the object motion is circular, the object motion model is (12) and we have

$$\begin{aligned} \ddot{z} &= J\ddot{q} + \lambda + N\omega + \Phi\omega^2, \\ \Phi &= F \begin{bmatrix} -s_{12} & c_{12} \\ c_{12} & s_{12} \end{bmatrix} \begin{bmatrix} -Y_{obj} \\ X_{obj} \end{bmatrix}, \\ N &= 2(\dot{q}_1 + \dot{q}_2)\Phi, \end{aligned} \quad (29)$$

where  $\lambda$  is given by (27). Thus the controller is

$$\tau = MJ^{-1}(-K_1 z - K_2 \dot{z} - \lambda - N\omega - \Phi\omega^2) + h. \quad (30)$$

## 5 Object Motion Estimation

Since the control law (25) and (26) requires  $\dot{z}$  and  $\theta^*$ , which are not usually known, an estimator for these parameters is needed. Let the estimates of the parameter

$\theta^*$  and controlled variable  $z$  be  $\hat{\theta}$  and  $\hat{z}$ , respectively, and consider the following estimator

$$\dot{\hat{z}} = J\dot{q} + LW\hat{\theta} + H(\hat{z} - z), \quad \dot{\hat{\theta}} = -W^T L^T P(\hat{z} - z), \quad (31)$$

where  $H$  is any stable matrix and  $Q$  is any positive definite matrix. While  $P$  is selected to satisfy

$$H^T P + PH = -Q, \quad Q > 0. \quad (32)$$

Let the estimation error vectors be

$$\bar{z} \stackrel{\text{def}}{=} z - \hat{z}, \quad \bar{\theta} \stackrel{\text{def}}{=} \theta^* - \hat{\theta}, \quad e \stackrel{\text{def}}{=} \begin{bmatrix} \bar{z} \\ \bar{\theta} \end{bmatrix}. \quad (33)$$

Then, we obtain the following theorem.

**Theorem 2** For all  $p \in \mathcal{U}$  and  $q \in \mathcal{V}$  the estimator (31) makes the equilibrium point  $e = 0$  asymptotically stable.

It is easy to prove this theorem by taking the Lyapunov function candidate as follows

$$V \stackrel{\text{def}}{=} e^T \tilde{P} e, \quad \tilde{P} \stackrel{\text{def}}{=} \begin{bmatrix} P & 0 \\ 0 & I \end{bmatrix}. \quad (34)$$

## 6 Observer-based Controller

Consider the following observer-based control law

$$\begin{aligned} \tau &= M(B^T J)^{-1}(v - \lambda - N\hat{\theta} - \Phi\kappa(\hat{\theta})) + h, \\ v &= -K_1 z - K_2 B^T (J\dot{q} + LW(p)\hat{\theta}). \end{aligned} \quad (35)$$

Defining  $\bar{\kappa} \stackrel{\text{def}}{=} \kappa(\theta^*) - \kappa(\hat{\theta})$  and substituting (35) into (22) yield

$$\ddot{z} = -K_1 z - K_2(\dot{z} - B^T LW\hat{\theta}) + N\bar{\theta} + \Phi\bar{\kappa}. \quad (36)$$

Thus we obtain the following closed loop dynamics

$$\dot{x} = \bar{A}x + \bar{N}\bar{\theta} + \bar{\Phi}\bar{\kappa}, \quad (37)$$

where  $x, \bar{A}, \bar{N}$  and  $\bar{\Phi}$  are defined by

$$\begin{aligned} x &\stackrel{\text{def}}{=} \begin{bmatrix} z \\ \dot{z} \end{bmatrix}, \quad \bar{A} \stackrel{\text{def}}{=} \begin{bmatrix} 0 & I \\ -K_1 & -K_2 \end{bmatrix}, \\ \bar{N} &\stackrel{\text{def}}{=} \begin{bmatrix} 0 \\ N + K_2 B^T LW \end{bmatrix}, \quad \bar{\Phi} \stackrel{\text{def}}{=} \begin{bmatrix} 0 \\ \Phi \end{bmatrix}. \end{aligned} \quad (38)$$

Finally we have the main theorem.

**Theorem 3** For the system (2), (3) and (9), estimator (31) and controller (35) make the equilibrium point  $(x, e) = 0$  asymptotically stable.

Though we omit the proof, it is straightforward based on the Lyapunov's method.

## 7 Simulation and Experiment

To show the effectiveness of the proposed estimator and controller, simulations are carried out on the two link planar robot illustrated in Figure 3 with  $\ell_1 = 300$ ,  $\ell_{cx} = 177$ ,  $\ell_{cy} = 88$  [mm]. Other parameters are as follows<sup>2</sup>: object position  $s_o = [282.5, -119, 2000]^T$  [mm], initial joint angle  $q = [-60, 80]^T$  [deg], initial object image  $\xi = [18, -20]^T$  [pixel] and the reference image  $\xi_d = [0, 0]^T$  [pixel]. The task is to track the object so that the object image is kept at the origin of the image plane.

### 7.1 Straight Motion

The object moved in  $X$  direction with 40 [mm/sec] at  $t = 6.5$  [sec], and stopped at  $t = 10.5$ ; moved again in  $Y$  direction with 20 [mm/sec] at  $t = 13.5$ , and stopped at  $t = 17$ . The results are shown in Figure 4. The horizontal axis is time; (a), (b) are feature errors; (c), (d) are estimates of the object speed. A white Gaussian noise with variance 0.1 [pixel<sup>2</sup>] was added to  $\xi$ . The solid line is the result with observer and the dotted line is the result without the observer (i.e.,  $\hat{\theta} \equiv 0$  in (35) [8]). The observer estimates the object speed very well and the controlled error is reduced considerably.

Experimental results are shown in Figure 5. The estimates are oscillatory compared with the simulation and the effect of oscillation is found in the controlled error, but the controlled error is fairly reduced.

### 7.2 Circular Motion

The second case is a circular motion with radius 20 [mm]. The object moved with angular velocity 2.8 [rad/sec] at  $t = 6.5$ ; changed the speed to 1.4 [rad/sec] at  $t = 17.5$ ; and stopped at  $t = 23.5$ . The simulation results are shown in Figure 6. The horizontal axis is time; (a), (b) are the feature errors; (c) is the estimate of the angular velocity. The observer works well and the controlled error is reduced considerably.

Experimental results are given in Figure 7. The controlled error is reduced, but it does not converge to zero because the measured center includes slight error.

## 8 Conclusion

We have proposed a visual feedback controller with a velocity estimator. We also have proved the asymptotical stability of the closed loop. Simulations on a two link planar robot exhibited the stable and accurate

<sup>2</sup>The object is above the robot and it moves in front of the camera which is looking upward.

performance. The effectiveness of the proposed scheme was evaluated by simulations and experiments.

## References

- [1] P. K. Allen, A. Timcenko, B. Yoshimi, and P. Michelman. Automated tracking and grasping of a moving object with a robotic hand-eye system. *IEEE Trans. Robotics and Automation*, 9(2):152–165, 1993.
- [2] F. Chaumette and A. Santos. Tracking a moving object by visual servoing. In *12th IFAC World Congress, Vol.9*, pages 409–414, Sydney, Australia, 1993.
- [3] P. I. Corke and M. C. Good. Controller design for high speed-performance visual servoing. In *12th IFAC World Congress, Vol.9*, pages 395–398, Sydney, Australia, 1993.
- [4] B. Espiau, F. Chaumette, and P. Rives. A new approach to visual servoing in robotics. *IEEE Trans. Robotics and Automation*, 8(3):313–326, 1992.
- [5] J. T. Feddema and O. R. Michell. Vision guided servoing with feature-based trajectory generation. *IEEE Trans. Robotics and Automation*, 5(5):691–700, 1989.
- [6] B. K. Ghosh, M. Lei, and E. P. Loucks. Visionics: A new vision guided estimation of a dynamical system. In *12th IFAC World Congress, Vol.9*, pages 415–418, Sydney, Australia, 1993.
- [7] K. Hashimoto et al. Manipulator control with image-based visual servo. In *IEEE Int. Conf. Robotics and Automation*, pages 2267–2272, Sacramento, Calif., 1991.
- [8] K. Hashimoto and H. Kimura. Dynamic visual servoing with nonlinear model-based control. In *12th IFAC World Congress, Vol.9*, pages 405–408, Sydney, Australia, 1993.
- [9] K. Hashimoto and H. Kimura. LQ optimal and nonlinear approaches to visual servoing. In *Visual Servoing, K. Hashimoto ed., World Scientific*, pages 165–198, Singapore, 1993.
- [10] A. J. Koivo and N. Houshangi. Real-time vision feedback for servoing robotic manipulator with self-tuning controller. *IEEE Trans. Systems, Man, and Cybernetics*, 21(1):134–142, 1991.
- [11] N. Papanikolopoulos, P. K. Khosla, and T. Kanade. Visual tracking of a moving target by a camera mounted on a robot: a combination of control and vision. *IEEE Trans. Robotics and Automation*, 9(1):14–35, 1993.
- [12] L. E. Weiss, A. C. Sanderson, and C. P. Newman. Dynamic sensor-based control of robots with visual feedback. *IEEE J. Robotics and Automation*, RA-3(5):404–417, 1987.
- [13] W. J. Wilson. Visual servo control of robots using Kalman filter estimates of relative pose. In *12th IFAC World Congress, Vol.9*, pages 399–404, Sydney, Australia, 1993.

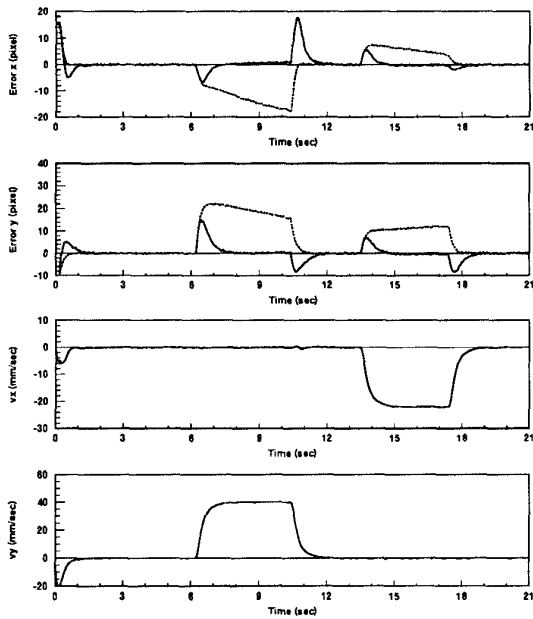


Figure 4: Simulation Results (Straight Motion)  
 (a)  $x$  Error (b)  $y$  Error  
 (c)  $X$  Estimated Velocity (d)  $Y$  Estimated Velocity  
 - -:Non-Adaptive —:Adaptive

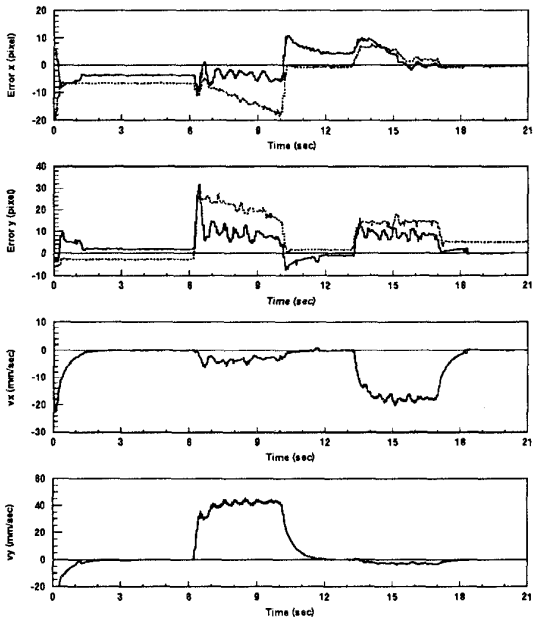


Figure 5: Experimental Results (Straight Motion)  
 (a)  $x$  Error (b)  $y$  Error  
 (c)  $X$  Estimated Velocity (d)  $Y$  Estimated Velocity  
 - -:Non-Adaptive —:Adaptive

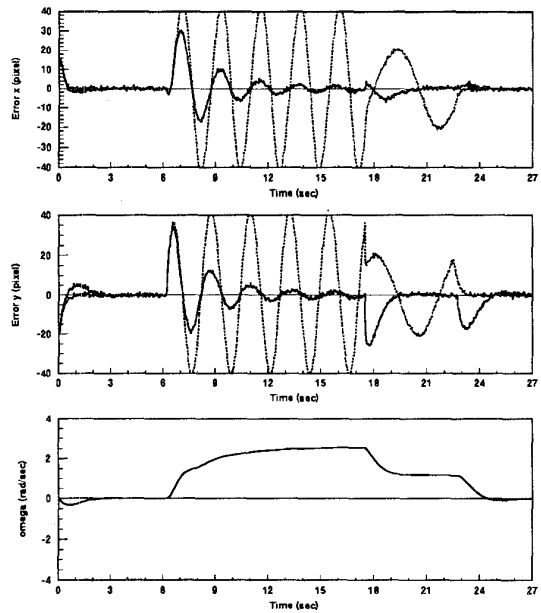


Figure 6: Simulation Results (Circular Motion)  
 (a)  $x$  Error (b)  $y$  Error  
 (c) Estimated Angular Velocity  
 - -:Non-Adaptive —:Adaptive

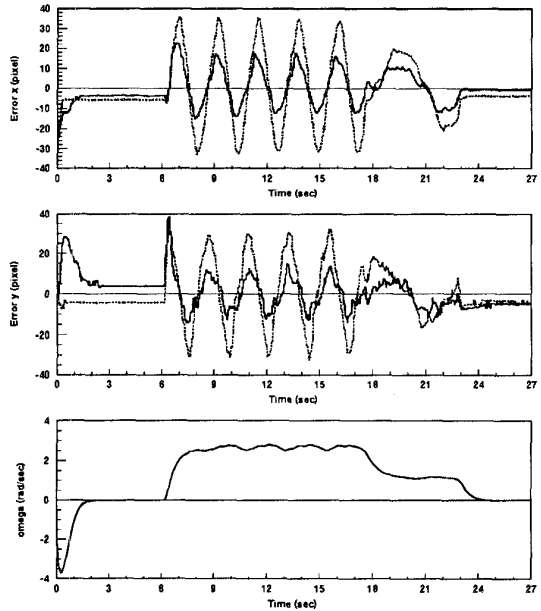


Figure 7: Experimental Results (Circular Motion)  
 (a)  $x$  Error (b)  $y$  Error  
 (c) Estimated Angular Velocity  
 - -:Non-Adaptive —:Adaptive